Chapter 12

Simulation of Walking

Frank C. Anderson, Allison S. Arnold, Marcus G. Pandy, Saryn R. Goldberg, and Scott L. Delp

Many elements of the neuromusculoskeletal system interact to enable walking. Scientists fascinated by human movement have performed an extensive range of studies to describe these elements, e.g., to identify the processes involved in neuromuscular activation, characterize the mechanics of muscle contraction, describe the geometric relationships between muscles and bones, and quantify the motions of joints. Clinicians who treat walking abnormalities in individuals with cerebral palsy, stroke, and other neuromusculoskeletal disorders have examined the electromyographic (EMG) patterns, gait kinematics, and ground reaction forces of literally thousands of patients, both before and after treatment interventions. However, synthesizing detailed descriptions of the neuromusculoskeletal system with gait measurements to create an integrated understanding of normal gait, to identify the sources of pathologic gait, and to establish a scientific basis for treatment planning remains a major challenge.

Using experiments alone to meet this challenge has two fundamental limitations. First, important variables, including the forces generated by muscles, are not readily accessible in experiments. Second, even when variables can be measured accurately, it is often difficult to establish cause-effect relationships. As a result, elucidating the functions of muscles from experiments is not straightforward. For example, ground reaction forces (see Chapter 4) can be measured and used to estimate the accelerations of the body's center of mass. However, force plate measurements alone offer little insight into how muscles contribute to these accelerations, and therefore to the critical tasks of supporting and propelling the body forward. EMG recordings (see Chapter 6) can indicate *when* a muscle is active, but examination of EMG recordings does not allow one to determine which motions of the body arise from a muscle's activity. Indeed, determining how individual muscles contribute to observed motions is not necessarily intuitive, as explained below, because a muscle can accelerate joints that it does not span and body segments that it does not touch (105).

A theoretical framework is needed, in combination with experiments, to advance our understanding of neuromusculoskeletal function during walking, e.g., to uncover the principles that govern the coordination of muscles during normal gait, to determine how neuromuscular impairments contribute to abnormal gait, and to predict the functional consequences of treatments. It is imperative that this framework reveals the cause-effect relationships between neuromuscular excitation patterns, muscle forces, ground reaction forces, and motions of the body. A dynamic simulation of walking that integrates facts about the anatomy and physiology of the neuromusculoskeletal system and the mechanics of multi-joint movement provides such a framework.

What is a dynamic simulation of movement, and how can it complement experimental studies of walking? A dynamic simulation is, in essence, a solution to a set of equations that describe how the forces acting on a system cause motions of the system over time, as governed by the laws of physics. A "muscle-driven" dynamic simulation of walking, therefore, describes how the forces produced by muscles (and other sources of force, such as gravity) contribute to motions of the body segments during the gait cycle.

The process for developing, testing, and analyzing a muscle-driven simulation of movement involves four stages (Figure 12-1). Stage 1 is to create a computer model that characterizes the dynamic behavior of the neuromusculoskeletal system with sufficient accuracy to answer specific research questions. The models that we, and others have developed typically include detailed descriptions of musculoskeletal geometry and equations that describe the activation and force production of muscles and the multi-joint dynamics of the body. Stage 2 is to find a set of muscle excitations which, when applied to the model, generate a simulation that reproduces the movement of interest. Stage 3 is to verify that the simulation is indeed representative of the movement of interest by comparing the results of the simulation to experimental data. Stage 4 is to analyze the simulation to answer the research or clinical questions posed.

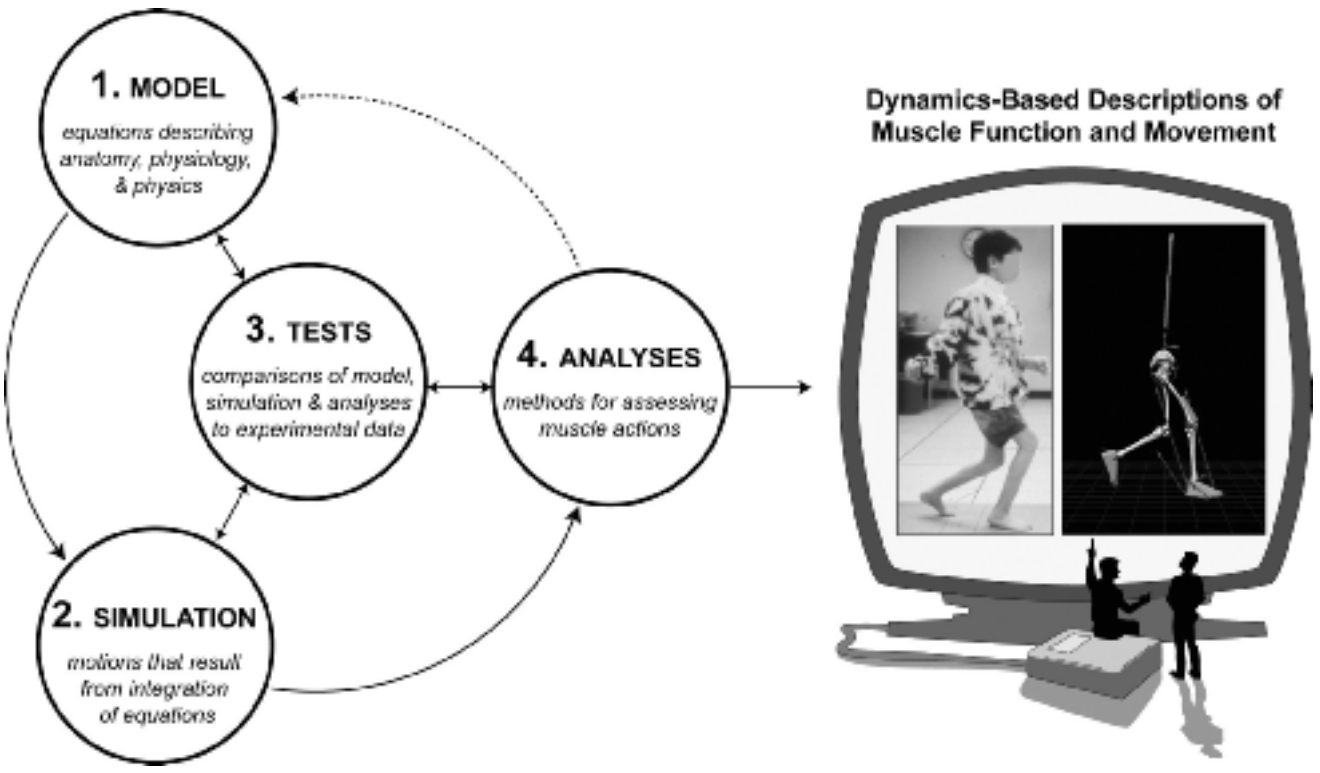

FIGURE 12-1. Stages involved in creating and analyzing a simulation of walking. A rigorous assessment of muscle function during walking requires (1) a model of neuromusculoskeletal dynamics, typically formulated as a set of equations that relate accelerations of the limb segments to the forces generated by muscles and other external forces, such as the force of gravity, (2) a simulation of the gait cycle, obtained by applying a set of muscle excitations to the model and integrating the equations of motion forward in time, (3) tests to verify that the simulation is sufficiently accurate to answer specific research questions, generally performed by comparing aspects of the model and simulation to experimental data, and (4) analyses of the simulation to determine how individual muscles generate forces and contribute to motions of the body.

A muscle-driven dynamic simulation provides unique capabilities that complement experimental approaches. Simulations provide estimates of important variables, such as muscle and joint forces, which are difficult to measure experimentally. Simulations also enable cause-effect relationships to be explained. For instance, the contribution that a muscle makes to the ground reaction force can be calculated. A simulation also allows "what if?" studies to be performed in which, for example, the excitation pattern of a muscle can be changed and the resulting motion can be observed. These capabilities provide new ways to characterize the functions of muscles during walking and other tasks.

Why are simulations needed to characterize the functions of muscles during walking? Simulations are needed because experimental approaches to infer a muscle's actions, based on the muscle's attachments, EMG activity, and measured motions of the body, do not explain how the forces produced by the muscle accelerate the body segments and contribute to motions of the joints. When a muscle applies a force to a segment, that segment is accelerated (Figure 12-2). The acceleration of the segment is resisted by the inertia of adjoining segments, giving rise to intersegmental forces at the joints. These intersegmental forces are transmitted from one segment to another due to the "coupled" multi-articular nature of the body. The transmission of these intersegmental forces, often referred to as *dynamic coupling*, means that a force applied to one body segment accelerates all body segments, not just the segment to which the force is applied. The relative magnitudes of the intersegmental forces at the joints depend, in part, on the mass and inertial properties of the segments being accelerated. For example, intersegmental forces at the hip that arise from accelerations of the thigh are generally greater than intersegmental forces at the metatarsophalangeal joints that arise from accelerations of the toes because the thigh is more massive than the toes. The magnitudes and directions of the intersegmental forces also depend on the applied muscle force and the configuration of the body.

How significant are the intersegmental forces induced by muscles during walking? In particular, are these forces

P1: NDK/OVY P2: NDK/OVY QC: NDK/OVY T1: NDK
GRBT092-12 Rose- 2252G GRBT092-Rose-v2.cls October 13, 2005 17:47

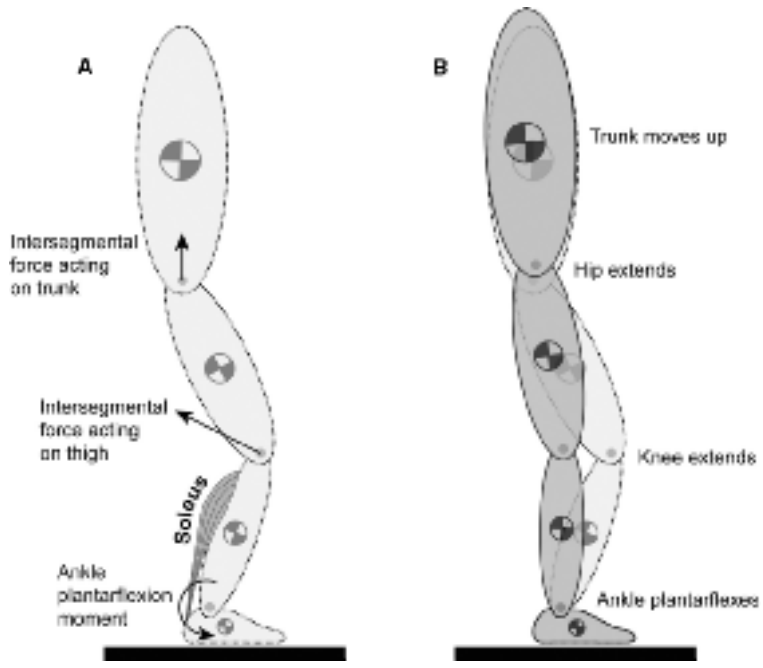

FIGURE 12-2. Dynamic actions of soleus during single-limb stance (knee flexion angle is exaggerated for the purpose of illustration). (**A**) The force applied by soleus, a uniarticular muscle spanning the ankle, not only generates an ankle plantarflexion moment (circular black arrow), but also induces intersegmental forces throughout the body. The magnitudes and directions of these intersegmental forces depend on the force applied by the muscle, the moment arms of the muscle, the inertial properties of the segments, and the configuration of the body. In this example, the force applied by soleus produces a counter-clockwise angular acceleration of the shank. This acceleration requires the location of the knee joint to accelerate to the left and upward. The inertia of the thigh resists this acceleration, resulting in an intersegmental force at the knee (straight black arrow). The intersegmental force at the knee accelerates the thigh, which in turn induces an intersegmental force at the hip (straight black arrow), and so on. (**B**) As a consequence of the intersegmental forces induced by soleus, soleus accelerates not only the ankle, but all the joints of the body. At the body position shown, soleus accelerates the ankle toward plantarflexion, the knee toward extension, the hip toward extension, and the trunk upward. Over time, these accelerations give rise to changes in position. Thus, due to dynamic coupling, soleus does not function solely as an "ankle plantarflexor"—in many situations, it likely does much more. In similar fashion, other muscles induce intersegmental forces and accelerate joints that they do not span.

large enough to influence our interpretation of the muscles' actions? The answer to this question, in many cases, is yes. Due to dynamic coupling, a muscular moment generated at one joint induces accelerations of that joint and other joints— including joints that the muscle does not span. These "muscle-induced" accelerations are generally small at joints far removed from the muscle; however, the induced accelerations of nearby joints can be substantial. For example, soleus exerts only an ankle plantarflexion moment, yet Zajac and Gordon (105) have demonstrated that soleus can accelerate the knee into extension more than it accelerates the ankle into plantarflexion. During the stance phase of normal gait (Figure 12-2), soleus accelerates both the knee and the ankle toward extension (9,45,56), an action commonly termed the *plantarflexion – knee extension couple* (33). The plantarflexion moment exerted by soleus during stance also accelerates the hip toward extension (9,45,58) and provides vertical support for the trunk (6,56,106). Based on this work and other examples, we believe that the effects of dynamic coupling must be considered when attempting to determine the functional roles of muscles during gait. Using a muscle-driven dynamic simulation, the intersegmental forces that result from a muscle's force can be calculated, and the resulting motions of the body segments can be quantified.

The remainder of this chapter summarizes our experiences with the development and analysis of muscle-driven simulations of human walking. There are many plausible approaches, and this chapter is not intended to be a comprehensive review. Rather, the chapter describes the development (Stages 1 and 2) and testing (Stage 3) of a particular simulation—a three-dimensional dynamic simulation of normal gait (5). Three studies are reviewed in

which this simulation was analyzed (Stage 4) to gain new insights into the functions of individual muscles during walking. The chapter concludes by summarizing some of the limitations of current modeling, simulation, and analysis techniques. Consideration of these limitations suggests future research.

STAGE 1: CREATING A DYNAMIC MODEL OF THE MUSCULOSKELETAL SYSTEM

In a muscle-driven dynamic simulation, elements of the neuromusculoskeletal system are modeled by sets of differential equations that describe muscle activation dynamics, musculotendon contraction dynamics, musculoskeletal geometry, and skeletal dynamics (Figure 12-3). These equations characterize the time-dependent behavior of the musculoskeletal system in response to neuromuscular excitation. Formulating these equations is the necessary first stage in generating a simulation (see also Pandy (67) for a review).

Muscles do not generate forces instantaneously in response to neuromuscular excitation (see also Chapter 6). Muscle activation dynamics, the time course of Ca^{++}–mediated activation of the contractile apparatus as modulated by motor unit action potentials, can be modeled by relating the time rate of change of muscle activation ($\dot{a}$) to muscle activation (a) and excitation (u):

$$\dot{a} = (u^2 - ua)/ \cdot \tau_{act} + (u - a)/\tau_{deact}, \qquad (1)$$

where τ_{act} and τ_{deact} are the time constants for activation and deactivation, respectively (62). Excitation and activation levels in Eq. 1 are allowed to vary continuously between zero (no excitation and activation) and one (full excitation and activation). Activation levels serve as inputs to the equations for musculotendon contraction dynamics that estimate muscle forces.

Musculotendon contraction dynamics, the time course of muscle force generation as determined by the energetics of cross bridge formation, the sliding of actin filaments, and the dynamics of tendon, can be modeled by relating the time rate of change of muscle force ($\dot{f}_M$) to musculotendon length (l_{MT}), musculotendon shortening velocity ($\dot{l}_{MT}$), and muscle activation (a):

$$\dot{f}_M = f(l_{MT},\ \dot{l}_{MT}, a), \qquad (2)$$

where the function $f(l_{MT}, \dot{l}_{MT}, a)$ characterizes the force-length-velocity properties of muscle and the force-length properties of tendon (66,107). The contraction dynamics of a particular muscle can be estimated by scaling the function by five parameters: maximum isometric muscle

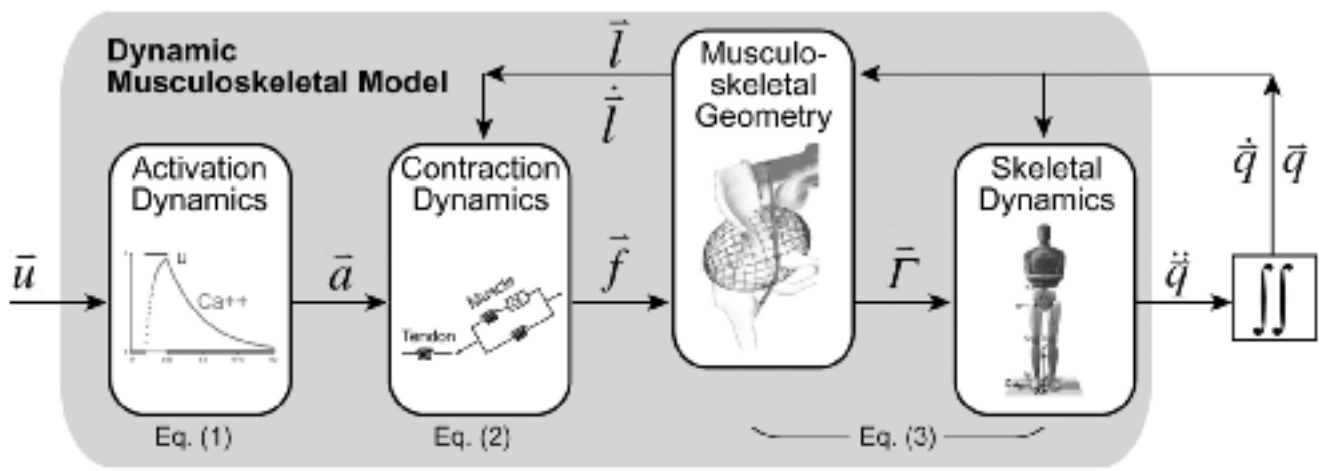

FIGURE 12-3. Elements of a muscle-driven simulation of walking. When a dynamic musculoskeletal model (shaded region) is driven by muscle excitations ($\vec{u}$), the resulting motions of the body, ($\ddot{\vec{q}}$, $\dot{\vec{q}}$, $\vec{q}$) can be calculated. The equation for muscle activation dynamics relates the muscle excitations to muscle activations ($\vec{a}$). The equations for musculotendon contraction dynamics relate the muscle activations to muscle forces (f); the muscle forces depend on musculotendon lengths and shortening velocities ($\vec{l}$, $\dot{\vec{l}}$). The muscle forces are transmitted to the skeleton resulting in joint torques ($\vec{\Gamma}$), which accelerate the limb segments according to the equations of motion that govern the multi-joint dynamics of the body. These accelerations ($\ddot{\vec{q}}$) depend on the mass and inertial characteristics of the limb segments, Coriolis and centrifugal forces, gravity, muscle forces, and any external forces produced when the body interacts with the environment. Equations 1–3 are numerically integrated forward in time to produce a simulation.

P1: NDK/OVY P2: NDK/OVY QC: NDK/OVY T1: NDK
GRBT092-12 Rose- 2252G GRBT092-Rose-v2.cls October 13, 2005 17:47

force and the corresponding muscle fiber length, maximum shortening velocity, pennation angle, and tendon slack length (i.e., the length at which tendon begins to transmit force when stretched). When applied to the skeleton, musculotendon forces act to accelerate the body segments.

The accelerations of the body segments in response to muscle forces and other loads can be computed from a description of the musculoskeletal geometry and the equations of motion that govern the multi-joint dynamics of the body:

$$\ddot{\vec{q}} = \overleftrightarrow{I}^{-1}(\vec{q}) \cdot \{\vec{G}(\vec{q}) + \vec{C}(\vec{q}, \dot{\vec{q}}) + \overleftrightarrow{R}(\vec{q}) \cdot \vec{f}_M + \vec{F}_E(\vec{q}, \dot{\vec{q}})\}. \quad (3)$$

In this set of equations, $\vec{q}$, $\dot{\vec{q}}$, and $\ddot{\vec{q}}$ are the generalized coordinates (e.g., joint angles), velocities, and accelerations of the model, respectively. $\overleftrightarrow{I}^{-1}$ is the inverse of the system mass matrix, which specifies the mass and inertial properties of the body segments. $\vec{G}$ is a vector of forces arising from gravity. $\vec{C}$ is a vector of forces arising from Coriolis and centrifugal forces, which are generated from the rotations of the body segments (e.g., like the forces encountered when swinging an object around in circles at the end of a rope). $\overleftrightarrow{R}$ is a matrix of muscle moment arms, and $\vec{f}_M$ is a vector of muscle forces. The muscle moment arms, or lever arms, determine the joint moments that result from application of the muscle forces. $\vec{F}_E$ is a vector of external forces that characterize the interactions with the environment.

We have used this general approach to create a model to simulate walking (4,5). The skeleton was represented as a 10 segment, 23 degree-of-freedom linkage (Figure 12-4). The pelvis was modeled as a rigid segment that was free to translate and rotate with respect to the ground. The remaining nine segments branched in an open chain from the pelvis. Segment masses, centers of masses, and moments of inertia were derived based on the regression equations reported by McConville et al (52) and anthropometric measures obtained from five healthy adult males. The equations of motion (Eq. 3) for the model were generated using a software package called SD/Fast (PTC, Needham, Massachusetts). Interactions between the feet and the ground were characterized using a series of spring-damper units distributed under the sole of each foot (i.e., $\vec{F}_E$ in Eq. 3). Torques representing the actions of ligaments were applied to the joints to prevent the joints from hyperextending during a simulation.

The model was driven by 54 musculotendon actuators. The path (i.e., line of action) of each actuator was specified based on anatomical landmarks (25). When an actuator wrapped around a bone or other muscles, via points and/or via cylinders were introduced to represent the path more accurately (26,35). Muscle activation dynamics were described using Eq. 1 with activation and deactivation

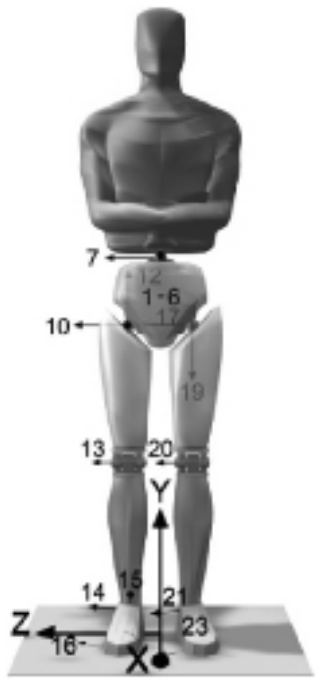

FIGURE 12-4. Skeletal degrees of freedom of the model. The head, arms, and torso were represented as a single rigid segment that articulated with the pelvis via a ball-and-socket joint located at approximately the third lumbar vertebra. Each hip was modeled as a ball-and-socket joint, each knee as a hinge joint, each ankle-subtalar joint as a universal joint, and each metatarsal joint as a hinge joint. Figure adapted from Anderson and Pandy (7).

time constants of 22 and 200 msec, respectively (66,107). Musculotendon contraction dynamics were described using Eq. 2 with musculotendon parameters based on data reported in the literature (18,25,31,97,107). Values of maximum isometric force and tendon slack length were adjusted for each actuator so that the isometric torque-angle curves for each joint in the model approximated the average torque-angle curves measured for five subjects (4). The model was completed when Eqs. 1–3 were formulated for the 54 musculotendon actuators and the 10 segment, 23 degree-of-freedom linkage.

STAGE 2: GENERATING A MUSCLE-DRIVEN SIMULATION OF WALKING

To generate a simulation of movement, the differential equations of a dynamic model are integrated forward in time (Figure 12-3). If the simulation is driven by muscles, a set of muscle excitations (i.e., u in Eq. 1) must be applied. A set of initial state variables (i.e., joint angles, joint angular velocities, muscle forces, and muscle activations at the initial time step) must also be specified. Integration

P1: NDK/OVY P2: NDK/OVY QC: NDK/OVY T1: NDK
GRBT092-12 Rose- 2252G GRBT092-Rose-v2.cls October 13, 2005 17:47

of the equations yields the time histories of all state variables in the model, including the muscle activations, musculotendon forces, and joint angles.

Finding a set of muscle excitations that produces a coordinated movement can be challenging. This is especially true for a movement as complex as walking. Not only must many degrees of freedom be controlled (e.g., 23 in the case of the musculoskeletal model described above), but also the time-dependent, nonlinear force-generating properties of muscle must be taken into account. To meet this challenge, dynamic optimization can be used (e.g., 4,5,23,44,55,56,65,103).

Dynamic optimization is a mathematical approach for finding a set of control values (e.g., the time histories of muscle excitations) for a dynamic system (e.g., a dynamic musculoskeletal model) that minimizes or maximizes a time-dependent performance criterion, possibly subject to constraints. To simulate walking or other multi-joint movements, a variety of performance criteria can be formulated. One approach is to solve an optimal tracking problem (e.g., 23,56). In this approach, the performance criterion is specified based on the difference between simulated and experimentally determined quantities, such as joint angles, joint powers, and ground reaction forces. By minimizing the performance criterion over the period of the simulation, the model is driven explicitly to reproduce experimental data. In other formulations, a set of muscle excitations might be found that minimizes or maximizes the model's performance of some hypothesized motor goal.

We have used this goal-based approach, in combination with the musculoskeletal model described above, to generate a muscle-driven simulation of walking (5). We hypothesized that the locomotor patterns of healthy individuals result from minimizing metabolic energy expenditure per unit distance traveled. This hypothesis is supported by measurements of metabolic energy consumption and observations of preferred walking speeds (76). The performance criterion (J) was therefore formulated as follows:

$$J = \frac{\int_0^{t_f} \dot{E}^M_{total}}{X_{cm}(t_f) - X_{cm}(t_i)} + penalty\ \ terms, \qquad (4)$$

where $\dot{E}^M_{total}$ is the rate at which total metabolic energy is consumed in the model and $X_{cm}(t_i)$ and $X_{cm}(t_f)$ denote the position of the model's center of mass at the initial and final times of the simulated gait cycle, respectively. The penalty terms were appended to increase the value of the performance criterion if any of the joints hyperextended during a simulation. $\dot{E}^M_{total}$ was computed by adding the basal metabolic heat rate of the whole body to the activation heat rate, maintenance heat rate, shortening heat rate, and the mechanical work rate of each muscle in the model. These rate terms were computed from the muscle activations, forces, shortening velocities, and other states of the model (16). To enforce repeatability of the gait cycle, we specified a number of terminal constraints. Specifically, the values of the joint angular displacements, joint angular velocities, muscle forces, and muscle activations at the end of the simulation were required to be the same as the values at the beginning. The values of the state variables at the beginning of the simulation were based on averaged experimental data.

Thus, the dynamic optimization problem that we solved was to find time histories of the muscle excitations that minimized J (Eq. 4) and met the constraints imposed to enforce repeatability. To solve this problem, we implemented a parameter optimization algorithm on parallel supercomputers (8,62). We applied the resulting muscle excitations to the dynamic model, integrated the equations of motion forward in time, and generated a simulation of walking. The locomotor pattern predicted by the optimal solution (Figure 12-5) successfully reproduced the salient features of normal gait.

STAGE 3: TESTING THE ACCURACY OF DYNAMIC SIMULATIONS

Before a simulation of movement can be analyzed, the simulation and the underlying model should be tested. In particular, it is important to verify that the dynamic behavior of the neuromusculoskeletal system is represented with sufficient fidelity to answer the research questions posed. For example, if the actions of individual muscles are of interest, the model should accurately characterize the muscle moment arms for the ranges of body positions assumed by the model during the simulation. Confidence in the muscle moment arms can be gained by comparing the moment arms predicted by the model to the moment arms determined experimentally from image data (e.g., 43) or from cadaveric specimens (e.g., 13,24). Confidence in the moment-generating capacities of muscles can be gained by comparing the maximum isometric joint moments generated by the model to the moments generated by human subjects (e.g., 4).

A simulation of movement can be tested by comparing quantities predicted by the simulation to quantities determined experimentally in the laboratory. For instance, the muscle excitation patterns, joint angles, joint moments, and ground reaction forces from a simulation of walking can be compared to EMG, kinematic, and kinetic data obtained from gait analysis. The similarity between predicted and measured values of metabolic energy consumption can also be assessed.

We have made detailed comparisons of the walking simulation, described above, to experimental data from five subjects (5). In most cases, the joint angles predicted by the simulation were within one standard deviation of the joint angles measured for the subjects. The simulated and

P1: NDK/OVY P2: NDK/OVY QC: NDK/OVY T1: NDK
GRBT092-12 Rose- 2252G GRBT092-Rose-v2.cls October 13, 2005 17:47

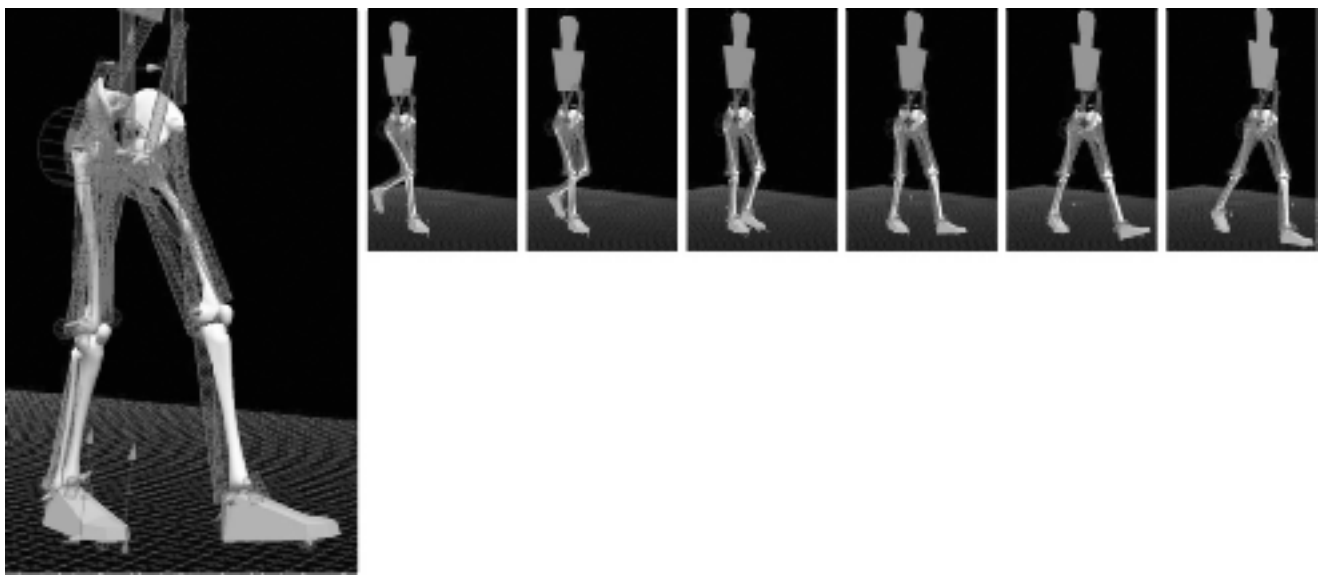

FIGURE 12-5. Snapshots of the muscle-driven simulation of walking obtained by solving a dynamic optimization problem.

measured ground reaction forces and muscle excitations also compared favorably (e.g., Figure 12-6). These tests provide some confidence that our simulation of walking reproduces the dynamics of normal gait (5).

STAGE 4: ANALYZING A SIMULATION OF WALKING

Once a muscle-driven simulation of movement is generated and tested, the simulation can be analyzed in several ways. Qualitatively, the motions produced from a particular set of muscle excitations can be visualized. Quantitatively, the contributions of individual muscles to the joint moments, joint angular accelerations, ground reaction forces, segmental energies, and other variables of interest can be determined. It is through the rigorous analysis and interpretation of such data that the value of a simulation can be realized.

The following examples demonstrate how a dynamic simulation can be analyzed to extract information about the actions of individual muscles during movement. Example 1 describes a method for decomposing the ground reaction force. We used this method to determine which muscles contribute to the vertical ground reaction force, and therefore to the vertical support of the body, during walking. Example 2 describes a technique for calculating the instantaneous angular accelerations of the joints induced by individual muscles during movement. We used this technique to determine which muscles are responsible for generating knee extension during the single-limb stance phase. Example 3 describes a method for quantifying how individual muscles (or other elements of a model) influence the motions of the body segments over time. We used this method to determine which muscles have the greatest potential to diminish knee flexion velocity prior to toe-off, a possible cause of stiff-knee gait. All three examples were generated using the dynamic optimization solution for walking described above.

Example 1: Decomposition of the Ground Reaction Force to Quantify Contributions to Support

The vertical ground reaction force is measured routinely, and its characteristic shape is well known for normal walking (Figure 12-6A). Because achieving adequate vertical support is one of the basic requirements of walking (42), quantifying how muscles contribute to the vertical ground reaction force, and therefore to the vertical acceleration of the center of mass, is an important part of our basic understanding of gait mechanics.

Several studies have examined how the shape of the ground reaction force is influenced by muscle activity (48,53,56,63,64,68,72,88,100). There has been broad consensus that the second maximum observed in the vertical ground reaction force is due largely to the forces exerted by the plantarflexors during late stance. However, an explanation for the shape of the ground reaction force during early stance and midstance has been less definitive. Muscles that potentially contribute have been inferred from experiments based on similarities between net joint moments and the shape of the ground reaction force (100), changes in the ground reaction force after the administration of nerve blocks (88), and the timing of muscle activity (72). However, without a theoretical framework for attributing portions of the ground reaction force to the forces produced by individual muscles, determining the relative

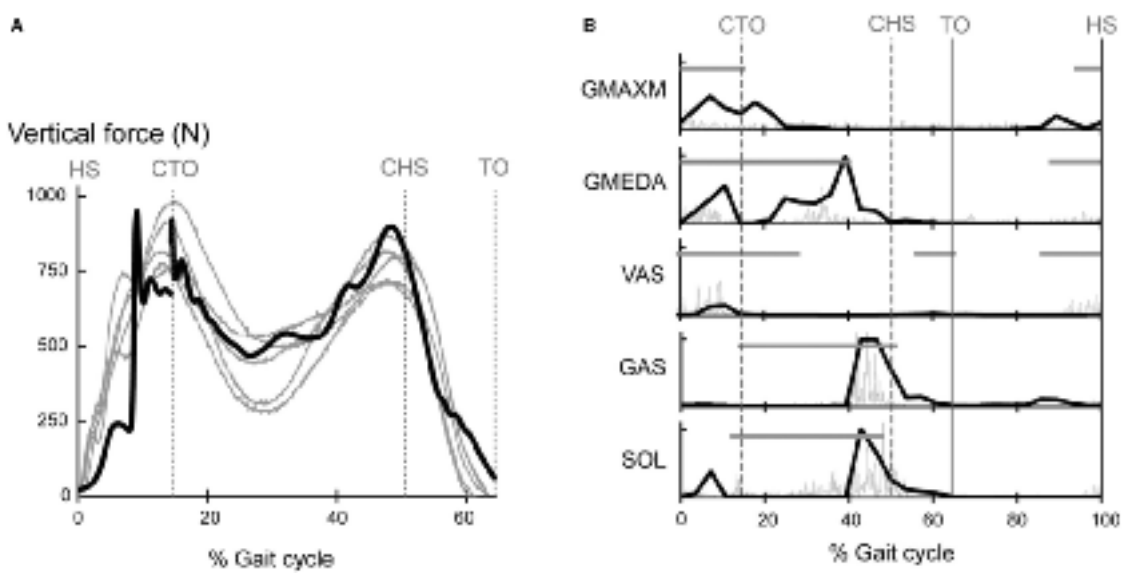

FIGURE 12-6. Tests of the muscle-driven simulation of walking. (**A**) The vertical ground reaction force generated during the simulation (*black line*) is representative of the ground reaction forces measured from five subjects during normal gait (*gray lines*). (**B**) The muscle excitation histories predicted by the dynamic optimization solution (black lines) compare favorably with EMG data recorded from one subject (gray lines) and with EMG data reported in the literature (horizontal gray bars) (75). The marked kinematic events are contralateral toe-off (CTO), contralateral heel-strike (CHS), toe-off (TO), and heel-strike (HS). (Figure adapted from Anderson and Pandy [5].)

contributions of muscles to the shape of the ground reaction force is difficult.

A number of studies (48,53,56) have used models of gait dynamics to estimate how muscles and other sources of force, such as gravity, contribute to the ground reaction force. This example summarizes the analyses we have performed to identify which sources of force make the largest contributions to the vertical ground reaction force, and therefore to support of the body during walking (6).

When interpreting experimental data obtained from gait analysis, it is often appealing to think of the ground reaction force as existing of its own accord, as a force to be balanced by net joint moments. Physically, however, the reverse is the case. "Reaction" forces, including the ground reaction force, arise as a consequence of "action" forces that act on and within the body. When muscles or other sources of force act on the body, they accelerate each foot with respect to the ground. Over time, these accelerations result in motion. When this motion brings a foot into contact with the ground, the foot and the ground deform (e.g., the compression of the sole of a shoe, or the depression of a wooden floor). Reaction forces are generated as a result of these deformations.

A muscle-driven dynamic simulation enables the cause-effect relationships between action forces, such as the forces produced by muscles, and reaction forces, such as the ground reaction force, to be established. Specifically, the ground reaction force generated during a simulation, $\vec{f}_E$, can be attributed to the Coriolis and centrifugal, gravity, ligament, and muscle forces that are applied:

$$\vec{f}_E = \vec{f}_E^C + \vec{f}_E^G + \vec{f}_E^L + \vec{f}_E^M, \tag{5}$$

where $\vec{f}_E^C$, $\vec{f}_E^G$, $\vec{f}_E^L$, and $\vec{f}_E^M$ are the contributions made to the ground reaction force by the Coriolis and centrifugal, gravity, ligament, and muscle forces, respectively. During walking, deformations of the foot and ground are small (i.e., typically much less than 1 cm), and $\vec{f}_E^C$, $\vec{f}_E^G$, $\vec{f}_E^L$, and $\vec{f}_E^M$ can be computed by assuming rigid contact between each foot and the ground. That is, when a foot contacts the ground, the component of the ground reaction force caused by a particular action force can be estimated by applying that action force to the model in isolation and calculating the reaction force needed to prevent the portion of the foot in contact with the ground from accelerating. The reaction force induced by a muscle, $\vec{f}_E^{M_i}$, for example, can be computed as the force necessary to prevent the foot from accelerating when muscle M_i alone acts on the body. We have used this method, in conjunction with our walking simulation, to generate a decomposition of the vertical ground reaction force throughout the stance phase (6).

Muscles made the largest contribution to vertical support in our simulation, accounting for 50% to 95% of the vertical ground reaction force generated in stance (Figure 12-7A, Muscle+Ligaments). The hip and knee extensors (gluteus maximus, posterior portion of gluteus medius, and vasti) were the main contributors to support in early stance, although prior to foot-flat the ankle dorsiflexors

P1: NDK/OVY P2: NDK/OVY QC: NDK/OVY T1: NDK
GRBT092-12 Rose- 2252G GRBT092-Rose-v2.cls October 13, 2005 17:47

made important contributions as well (Figure 12-7B). The hip abductors (anterior and posterior portions of gluteus medius and minimus) were the main contributors to support in midstance (Figure 12-7C). The ankle plantarflexors (primarily soleus and gastrocnemius) were the main contributors to support in late stance (Figure 12-7D). The passive transmission of force through the joints and bones in resistance to gravity accounted for 20% to 50% of the ground reaction force when the foot was flat on the ground, but made much smaller contributions before foot-flat and after heel-off (Figure 12-7A, Gravity). Coriolis and centrifugal forces acted to reduce the ground reaction force, but these contributions were far less than the contributions made by muscles or gravity (Figure 12-7A, Coriolis and Centrifugal).

Thus, by analyzing the cause-effect relationships between muscle forces and ground reaction forces during walking, a quantitative picture of how muscles contribute to the shape of the vertical ground reaction force has emerged. The first maximum in the ground reaction force results from the actions of the hip and knee extensors; the second maximum from the ankle plantarflexors. These muscles, along with the hip abductors, are the predominant contributors to vertical support during normal gait. The skeleton offers some support in resistance to gravity, but this support is less than 50% of body weight.

The methodology described in this example has numerous applications. By analyzing a simulation of a patient's abnormal gait, for instance, it may be possible to link deviations in the ground reaction force to the actions of particular muscles, perhaps identifying the cause of the patient's gait abnormality. In addition, as described in the next example, performing a decomposition of the ground reaction force is necessary for calculating the accelerations of the joints induced by individual muscles.

Example 2: Induced Acceleration Analysis to Quantify Muscle Actions in Single-Limb Stance

Children with cerebral palsy frequently walk with excessive knee flexion during the stance phase. This movement abnormality, called crouch gait, is problematic because it increases patellofemoral force (69), impedes toe clearance, and dramatically increases the energy requirements of walking (19,81,87). The persistent knee flexion typically worsens if left uncorrected (32,89) and can lead to altered patellofemoral joint mechanics and chronic knee pain (17,50,82,90).

Unfortunately, the biomechanical causes of crouch gait are often unclear, making it challenging to determine the most appropriate treatment. In some cases, abnormally "short" or "spastic" hamstrings are presumed to limit knee extension, and surgical lengthening of the hamstrings is performed (1,17,29,70). In other cases, diminished plantarflexion strength is thought to be a factor, and ankle-foot orthoses are prescribed (34,79). Other hypothesized causes

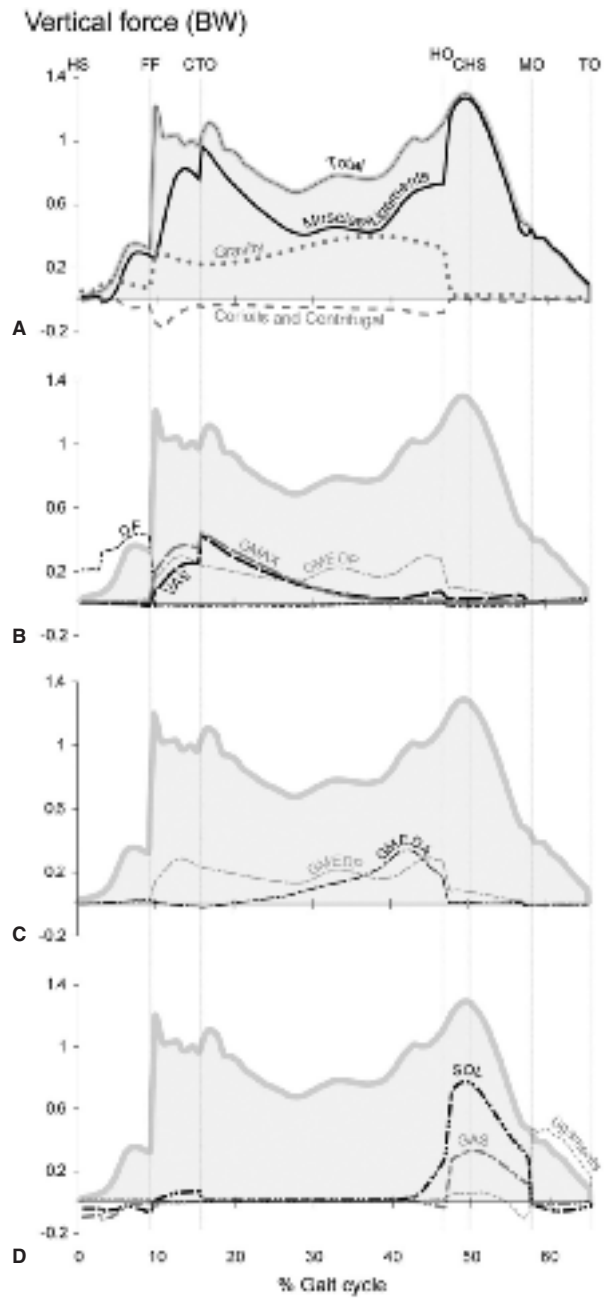

FIGURE 12-7. Decomposition of the ground reaction force during normal gait. (**A**) Contributions made to the ground reaction force by muscle and ligament forces (Muscles + Ligaments), Coriolis and centrifugal forces (Coriolis and Centrifugal), and resistance to gravity provided by the bones and joints of the skeleton (Gravity). Contributions made to the ground reaction force (**B**) during early stance by the dorsiflexors (DF), vasti (VAS), gluteus maximus (GMAX), the posterior portion of gluteus medius and minimus (GMEDP), (**C**) during mid-stance by the posterior and anterior portions of gluteus medius and minimus (GMEDA and GMEDP, respectively), and (**D**) during late stance by soleus (SOL), gastrocnemius (GAS), and the ligaments (Ligaments). The marked kinematic events are heel-strike (HS), foot-flat (FF), contralateral toe-off (CTO), heel-off (HO), contralateral heel-strike (CHS), metatarsal-off (MO), and toe-off (TO). (Figure adapted from Anderson and Pandy [(6]).

of crouch gait include malrotation of the femur, tibia, and foot (34,85), tight hip flexors (17,60,77,80), weak hip extensors (98), weak knee extensors (15,22,34), and poor balance (32).

Successful treatment of crouch gait is difficult, in part, because the factors that contribute to knee extension during normal gait are not well understood, and because the potential of individual muscles to produce knee flexion or extension during the stance phase is unknown. Knee motions are influenced not only by muscles that cross the knee, but also by muscular moments that are generated at other joints. To understand how knee extension is achieved during normal gait, and to elucidate the factors that potentially contribute to crouch gait, the effects of dynamic coupling must be considered. That is, the intersegmental forces that arise from a muscle's force must be computed, and the resulting multi-joint accelerations of the body must be evaluated.

We have used the simulation of walking, described above, to quantify the angular accelerations of the knee induced by the gluteus maximus, hamstrings, vasti, soleus, and other muscles during single-limb stance (9). This example illustrates how a simulation can be analyzed to reveal the dynamic actions of individual muscles during movement.

We determined the muscle-induced accelerations of the knee using the equations of motion for the model (Eq. 3) and the decomposition of the ground reaction force described in Example 1. At each time step in the simulation, a muscle's contributions to the instantaneous accelerations of the generalized coordinates ($\ddot{\vec{q}}_{M_i}$) were computed by applying that muscle's force ($\vec{f}_{M_i}$), as generated during the simulation, and the corresponding portion of the ground reaction force induced by that muscle ($\vec{f}_E^{M_i}$):

$$\ddot{\vec{q}}_{M_i} = \overleftrightarrow{I}(\vec{q})^{-1} \cdot \left\{ \overleftrightarrow{R}(\vec{q}) \cdot \vec{f}_{M_i} + \overleftrightarrow{E}(\vec{q}) \cdot \vec{f}_E^{M_i} \right\} \qquad (6)$$

All other forces in the model were set to zero. $\overleftrightarrow{E}$ is a matrix that converts the foot-ground spring forces into generalized forces (46).

Two descriptions of the muscle actions during single-limb stance were examined. First, the angular accelerations of the knee induced by individual muscles were quantified to determine which of the muscles enabled knee extension in the simulation of normal gait. Second, the muscle-induced accelerations of the knee per unit force were calculated to assess the "dynamic potential" of each muscle to accelerate the knee toward flexion or extension. This measure of a muscle's actions (obtained by setting $\vec{f}_{M_i} = 1\text{N}$, computing the corresponding $\vec{f}_E^{M_i}$, and substituting these quantities into Eq. 6) does not depend on the muscle excitations or forces applied during the simulation; rather, it reflects the influence of a muscle's moment arms and the inertial properties of the body. Hence, this analysis evaluated the relative potential of a muscle to generate (or limit) knee extension if, for example, the muscle was activated inappropriately or was producing excessive passive force.

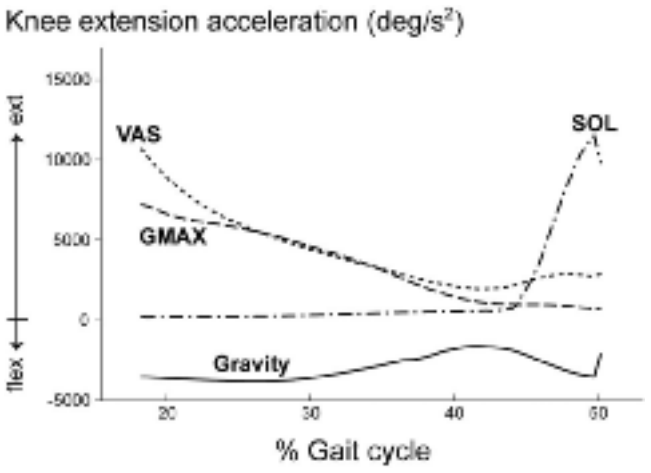

FIGURE 12-8. Contributions of vasti (VAS), gluteus maximus (GMAX), soleus (SOL), and gravity to the angular accelerations of the knee during the single-limb stance phase of normal gait. Gravity, together with its contribution to the ground reaction force, accelerated the knee toward flexion. The effects of gravity were resisted by muscles crossing the hip, knee, and ankle.

Examination of the muscle-induced accelerations showed that the gluteus maximus, vasti, soleus, and posterior portion of the gluteus medius made substantial contributions to knee extension during normal gait (Figure 12-8). Per unit force, the gluteus maximus had greater potential than the vasti to accelerate the knee toward extension (Figure 12-9). These data suggest that diminished force in the hip extensors, knee extensors, or ankle plantarflexors

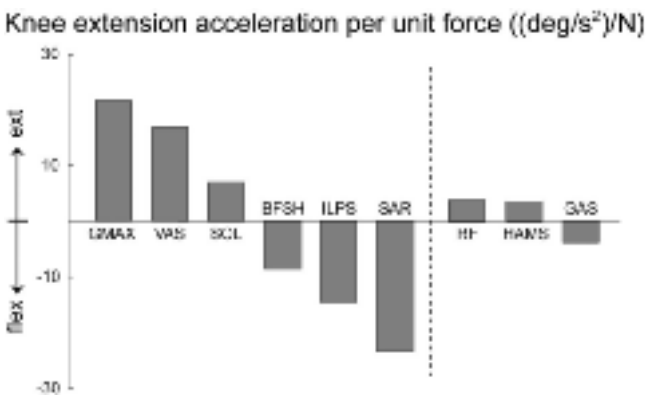

FIGURE 12-9. Angular accelerations of the knee per unit force, averaged over the single-limb stance phase (17%–50% of the gait cycle), induced by gluteus maximus (GMAX), vasti (VAS), soleus (SOL), biceps femoris short head (BFSH), iliopsoas (ILPS), sartorius (SAR), rectus femoris (RF), hamstrings (HAMS), and gastrocnemius (GAS).

P1: NDK/OVY P2: NDK/OVY QC: NDK/OVY T1: NDK
GRBT092-12 Rose- 2252G GRBT092-Rose-v2.cls October 13, 2005 17:47

may contribute to crouch gait, and strengthening these muscles, particularly the gluteus maximus, may help to improve both hip and knee extension. Abnormal forces generated by spasticity or contracture of the iliopsoas may also cause crouch gait in some cases, since these muscles have a large potential to accelerate the knee toward flexion (Figure 12-9).

The potential of the biarticular hamstrings, rectus femoris, and gastrocnemius muscles to induce angular accelerations of the knee during single-limb stance was small relative to other muscles (Figure 12-9). This was caused by dynamic coupling. Each of these muscles generated a moment about the knee and a moment about an adjacent joint, and these moments induced opposing accelerations of the knee. For example, the knee flexion moment generated by hamstrings acted to accelerate the knee toward flexion, but the hip extension moment generated by hamstrings acted to accelerate the knee toward extension. During the stance phase, in fact, the hamstrings had the potential to weakly accelerate the knee toward *extension* in our model. This occurred because the hamstrings' hip extension moment accelerated the knee toward extension more than the hamstrings' knee flexion moment accelerated the knee toward flexion. This unexpected result suggests that abnormally short or spastic hamstrings, a reputed cause of crouch gait, may not be the direct source of excessive knee flexion in some patients.

Our analysis of the muscle-induced accelerations of the knee, as described in this example, has clarified some of the actions of muscles during walking and has identified factors that are likely to contribute to excessive knee flexion in persons with cerebral palsy. This work emphasizes the need to consider how muscular forces contribute to multijoint movement when attempting to identify the causes of a patient's abnormal gait. Another method for characterizing the actions of muscles during movement is described in the next example.

Example 3: Perturbation Analysis to Quantify Muscle Actions in Double Support

Knee flexion velocity at toe-off is an important factor in generating swing-phase knee flexion during normal gait (53,73). Low knee flexion velocity at toe-off is a potential contributor to stiff-knee gait, a movement abnormality associated with stroke and cerebral palsy in which swing-phase knee flexion is diminished. Stiff-knee gait is commonly attributed to excessive activity of the rectus femoris, which is thought to limit knee flexion by producing an excessive knee extension moment during swing (71,91). However, we have shown that many individuals with stiff-knee gait do not exhibit excessive knee extension moments during swing phase, but instead walk with a low knee flexion velocity at toe-off (38). During normal gait, just prior to toe-off, knee flexion velocity increases dramatically during double support. If the muscles that produce angular accelerations of the knee during double support were known, then perhaps treatments to correct stiff-knee gait could be designed more effectively.

Comparisons of EMG recordings and measured gait kinematics have suggested that gastrocnemius, popliteus, and occasionally gracilis contribute to knee flexion during the late stance phase (72). Rectus femoris (72) and, in some cases, vasti (101) are also active during this period and are thought to limit knee flexion. However, the potential of these and other muscles to produce knee flexion or extension during walking cannot be deduced from kinesiologic observations alone. We have used the muscle-driven simulation of walking, described above, to identify the muscles that influence knee flexion velocity during double support and to determine which muscles have the greatest potential to alter this velocity (37).

In a muscle-driven simulation, joints are accelerated because of muscle forces. If a muscle's force is altered, or "perturbed," by a small amount during a simulation, the resulting changes in the motions of the joints can be quantified (i.e., by reintegrating the equations of motion forward in time). This technique, called perturbation analysis, is useful for investigating how individual muscles or other elements of a model influence the angular displacements and velocities of the joints. We used this technique in this example.

We quantified the actions of individual muscles in our simulation by systematically perturbing each muscle's force in double support and calculating the resulting changes in peak knee flexion velocity (Figure 12-10). We altered the muscle forces in two ways. First, we increased the force in each muscle by a percentage of the muscle's unperturbed force. The resulting change in knee flexion velocity depended on the muscle's unperturbed force and characterized how much that muscle's force influenced peak knee flexion velocity during the simulation. Second, we increased the force in each muscle by a fixed amount in Newtons. Using this approach, the resulting change in knee flexion velocity per unit force was independent of the muscle's unperturbed force, and characterized the potential of the muscle to influence knee flexion velocity based on the muscle's moment arms and the inertial properties of the body.

Analysis of the simulation revealed that iliopsoas and gastrocnemius were the largest contributors to peak knee flexion velocity during double support (Figure 12-11A). Each of these muscles exerted relatively large forces in the simulation, and each had a large potential to increase knee flexion velocity (Figure 12-11B). The forces generated by vasti, soleus, and rectus femoris, by contrast, decreased knee flexion velocity (Figure 12-11A). Vasti decelerated knee flexion the most. This is because vasti had the largest potential to decrease knee flexion velocity (Figure 12-11B), and because these muscles developed passive forces during double support. Soleus also exerted large forces

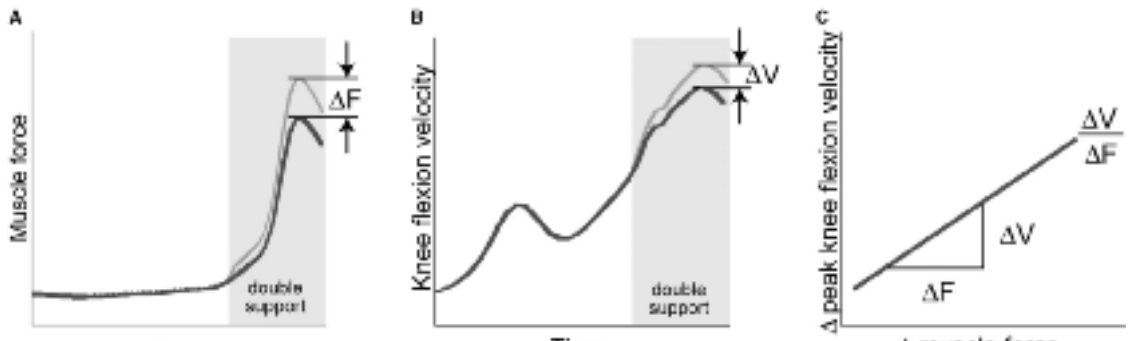

FIGURE 12-10. Steps to assess muscle function in a perturbation analysis. (**A**) A perturbation in an individual muscle force was introduced during the period of double support. (**B**) A dynamic simulation was performed with this altered muscle force and the resulting change in peak knee flexion velocity during double support was observed. (**C**) After repeating steps A) and B) for a range of perturbation sizes, the change in peak knee flexion velocity was plotted vs. the size of the force perturbation. The resulting slope was computed for different muscles to assess the relative influence of these muscles on knee flexion velocity.

during double support, but had a small potential relative to vasti to decrease knee flexion velocity (Figure 12-11B).

The muscles with the greatest potential to increase knee flexion velocity during double support, per unit force, were sartorius and gracilis (Figure 12-11B). When activated, these muscles generate hip flexion moments and knee flexion moments, both of which promote knee flexion. Biceps femoris short head, a uniarticular knee flexor, also had a relatively large potential to increase knee flexion velocity.

These analyses have advanced our understanding of muscle function during normal gait, and have helped to identify several possible causes of stiff-knee gait. In particular, our results suggest that insufficient force in iliopsoas or gastrocnemius, or excessive force in vasti or rectus femoris could limit knee flexion velocity during double support, and cause swing-phase knee flexion to be diminished. The stance-phase actions of these and other muscles, such as gracilis, should be considered before performing muscle-tendon surgery to treat stiff-knee gait.

CHALLENGES AND FUTURE DIRECTIONS

The first muscle-driven simulation of walking was developed more than three decades ago by Chow and Jacobson (21). Their dynamic model consisted of a single leg confined to the sagittal plane that was driven by four

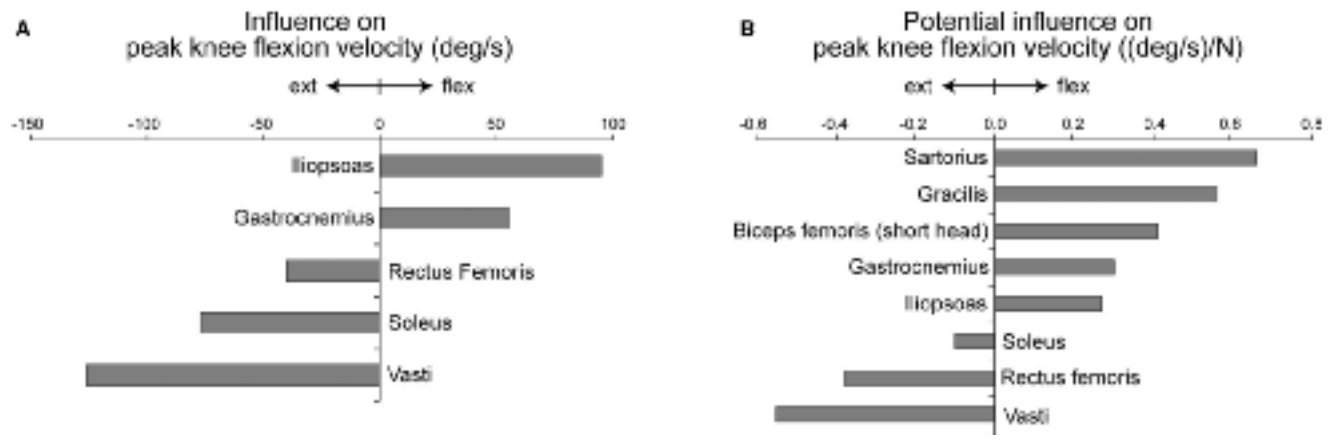

FIGURE 12-11. The muscles with the most influence and the most potential to influence peak knee flexion velocity. (**A**) The influence of selected muscles on the peak knee flexion velocity during double support. The influence was calculated as the slope of the change in peak knee flexion velocity (ΔV) vs. perturbation size as a percentage of unperturbed muscle force (ΔF) throughout the period of double support. (**B**) The potential influence of selected muscles on the peak knee flexion velocity during double support. These values characterize the change in peak knee flexion velocity (ΔV) due to a 1 N change in muscle force (ΔF) throughout the period of double support. (Figure adapted from Goldberg, et al.) (37).

P1: NDK/OVY P2: NDK/OVY QC: NDK/OVY T1: NDK
GRBT092-12 Rose- 2252G GRBT092-Rose-v2.cls October 13, 2005 17:47

idealized muscles. Nearly two decades passed before Davy and Audu (23) and then Yamaguchi and Zajac (104) published significantly advanced muscle-driven simulations of walking. Over the last few years, there has been a dramatic increase in the number and complexity of walking simulations, enabled, in large part, by new modeling software and increases in computer speed. To date, simulations of normal gait have been developed and analyzed to estimate the forces produced by muscles (e.g., 7), to determine how individual muscles support the body (56,58), accelerate the joints (44,45), and distribute energy among the limb segments (58,59), and to evaluate theories of neuromotor control (36,40,61,92,106). Muscle-driven simulations have also been created and used to evaluate exercise protocols for persons with spinal cord injury (84) and patients with patellofemoral pain (57), to examine the influence of foot positioning and joint compliance on the occurrence of ankle sprains (102), to assess computational prototypes of knee implants (74), and to investigate causes of stiff-knee gait (3,37,73,78). These studies, and the examples presented in this chapter, demonstrate the utility of muscle-driven simulations for elucidating the functions of muscles during movement and, potentially, improving the outcomes of treatments for persons with neuromusculoskeletal impairments.

Although models of the musculoskeletal system have become more sophisticated and novel approaches for analyzing simulations have been developed, rigorous dynamics-based techniques for determining which impairments contribute to the abnormal gait patterns of persons with neuromusculoskeletal disorders do not exist. We believe that the limitations of current models and analyses must be addressed before simulations can be widely used to guide treatment decisions for patients. Some of the important issues to be resolved in future studies are outlined below.

Modeling Challenges

Models that more accurately and efficiently characterize the musculoskeletal geometry and the joint kinematics of individual subjects need to be developed. This is imperative because the results of simulations are often sensitive to the accuracy with which the lengths and moment arms of muscles can be estimated. Studies of muscle function during walking have typically relied on "generic" models of adult subjects with normal musculoskeletal geometry. We have modified generic models to represent bone deformities (10-12), osteotomies (30,83), and tendon transfer surgeries (27). However, more work is needed to understand how variations in musculoskeletal geometry due to size, age, deformity, or surgery might influence the predictions of a model, and to determine when, and under what conditions, simulations based on generic models are applicable to individual patients. One approach might be to develop subject-specific models from magnetic resonance images or ultrasonography scans (e.g., 43,51,86,99). However, this approach may not always be practical. An alternative approach that combines medical images with generic musculoskeletal models, we believe, offers a promising, tractable way to construct models that are representative of patients. For instance, it may be possible to transform a generic model to represent a range of individuals with cerebral palsy using multi-dimensional scaling techniques, algorithms for deforming bones, and a few subject-specific parameters derived from image data or experimental measurements (11,20). We have begun to develop and evaluate such models (10,11), and we believe that additional efforts are warranted.

The equations for musculotendon dynamics that we have used in simulations must be further tested. While existing models capture many features of muscle force generation in unimpaired subjects, they do not account for adaptations that can occur in persons with neuromuscular disorders or alterations that might occur after surgery. We have developed models that attempt to account for decreases in the muscle fiber lengths that may occur with contracture (28). However, muscle-tendon models that account for structural changes in the extracellular matrix that may occur with chronic spasticity (49), or alterations in force transmission due to scar tissue (14) are not yet generally available. Muscle-tendon models that characterize the effects of pathology, surgery, and other treatment modalities on the time course of muscle force generation are needed to assess the impact of these effects on movement and neuromotor control.

Simulation Challenges

Using dynamic optimization to determine the muscle excitation patterns needed to simulate complex three-dimensional movements, such as walking, incurs great computational expense. The dynamic optimization solution for normal walking presented in this chapter required over 5000 computer processor hours to compute, and relied heavily on the use of parallel supercomputers (5). Although approaches for solving dynamic optimization problems are improving (41,47,54,96), this process is still very slow— at best, a solution for pathological gait might be obtained in a few days or a week. If dynamic simulations are to guide treatment decisions, then efficient computational algorithms for generating subject-specific simulations must be developed.

Fortunately, alternatives to dynamic optimization are emerging. Adaptations of traditional robotics control techniques appear to be particularly promising (e.g., 93,95). A technique called computed muscle control, for example, has been used to generate a simulation of bicycle pedaling approximately 100 times faster than conventional dynamic optimization approaches (93). We believe that

this technique will soon enable subject-specific simulations of walking to be generated in a few minutes.

Perhaps the most profound limitation of the simulation of walking described in this chapter is its exclusion of the nervous system. The simulation was performed open loop; that is, the muscle excitations were not modulated by reflexes. This is true of most dynamic simulations of movement generated to date, particularly those involving the lower extremity. However, simulations that are driven by neural networks and/or central pattern generators, that include simplified models of the nervous system, are being developed (e.g., 39,61,92). The incorporation of accurate representations of sensory-motor control (e.g., 94) into dynamic simulations of abnormal movements is one of the most critical challenges to be overcome if models are to be developed that can predict the outcomes of treatments.

Analysis Challenges

Characterizing the functions of muscles and extracting the principles that govern muscle coordination from dynamic simulations is nontrivial. Three approaches for quantifying the actions of muscles were illustrated in this chapter, but each of these analyses has limitations. Our method for decomposing the ground reaction force, as performed in Example 1, assumes rigid contact between the foot and the ground. To the extent that contact is not rigid, a portion (usually a small portion) of the reaction force cannot be explained (2). Calculations of muscle-induced accelerations, as performed in Example 2, rely on an accurate decomposition of the ground reaction force, and depend on the degrees of freedom that are included (or not included) in the model. Perturbation analysis, as performed in Example 3, provides an intuitive method for assessing how a muscle influences movement (i.e., not just accelerations, but also velocities and positions) by altering muscle force and quantifying the changes in movement over time. However, the results of perturbation analyses can be misleading if the perturbations in muscle force are too large or if the time windows over which perturbations are applied are too long. We believe that improved methods for analyzing simulations will evolve by applying these and other techniques to a range of research problems and critically evaluating the results.

Experimental observations and a theoretical framework are needed to establish a scientific basis for the treatment of gait abnormalities. Before a simulation of walking can be used to make treatment decisions, the simulation and the underlying model must be tested. If possible, simulation results should be compared with experimental data to verify that a particular simulation is of sufficient fidelity to answer the clinical question being posed. Sensitivity studies must be performed to determine whether the conclusions drawn from analysis of a simulation are sensitive to variations in model parameters, especially if a direct comparison with experimental data is not feasible. Ultimately, controlled clinical studies are required to determine if the insights gained from simulations can indeed improve treatment outcomes.

Experiments and Theory

We believe that a comprehensive explanation for how muscles are coordinated to produce gait is emerging. This belief is supported by the convergence of findings between some experimental and theoretical studies. For instance, it was no surprise in Example 1 that the plantarflexors are largely responsible for the second maximum in the vertical ground reaction force (Figure 12-7D); this was inferred previously from several experimental studies, and a number of simulations have confirmed a cause-effect relationship. Other results from our simulation-based analyses of walking are more surprising. For example, our finding that hamstrings weakly accelerate the knee toward extension during stance (Example 2, Figure 12-9) was unexpected. It is the unexpected findings from simulations, and the reconciliation of these findings with what we believe we already know from experiments, that have the potential to deepen our understanding of walking.

With the development, analysis, and testing of muscle-driven dynamic simulations, we are now in a position to establish quantitative, cause-effect relationships between the neuromuscular excitation patterns, muscle forces, ground reaction forces, and motions of the body that are observed in the laboratory. Coupled with high quality experimental measurements, dynamic simulations will be used to elucidate how the elements of the neuromusculoskeletal system interact to produce movement and, we hope, improve the outcomes of treatments for persons with movement disorders.

REFERENCES

1. Abel MF, Damiano DL, Pannunzio M, Bush J. Muscle-tendon surgery in diplegic cerebral palsy: Functional and mechanical changes. *J Pediatr Orthop* 1999;19:366–375.
2. Anderson FC, Arnold AS, Delp SL. Reaction forces induced by muscles in the presence of compliant contact. *Proceedings from the 4th World Congress of Biomechanics*, 2002.
3. Anderson FC, Goldberg SR, Pandy MG, Delp SL. Contributions of muscle forces and toe-off kinematics to peak knee flexion during the swing phase of normal gait: An induced position analysis. *J Biomech* 2004;37:731–737.
4. Anderson FC, Pandy MG. A dynamic optimization solution for vertical jumping in three dimensions. *Comput Methods Biomech Biomed Engin* 1999;2:201–231.
5. Anderson FC, Pandy MG. Dynamic optimization of human walking. *J Biomech Eng* 2001;123:381–390.
6. Anderson FC, Pandy MG. Individual muscle contributions to support in normal walking. *Gait Posture* 2003;17:159–169.
7. Anderson FC, Pandy MG. Static and dynamic optimization solutions for gait are practically equivalent. *J Biomech* 2001;34:153–161.
8. Anderson FC, Ziegler JM, Pandy MG, Whalen RT. Application of high-performance computing to numerical simulation of human movement. *J Biomech Eng* 1995;117:155–157.

9. Arnold AS, Anderson FC, Pandy MG, Delp SL. Muscular contributions to hip and knee extension during the stance phase of normal gait: A framework for investigating the causes of crouch gait. In press.
10. Arnold AS, Blemker SS, Delp SL. Evaluation of a deformable musculoskeletal model for estimating muscle-tendon lengths during crouch gait. *Ann Biomed Eng* 2001;29:263–274.
11. Arnold AS, Delp SL. Rotational moment arms of the medial hamstrings and adductors vary with femoral geometry and limb position: Implications for the treatment of internally-rotated gait. *J Biomech* 2001;34:437–447.
12. Arnold AS, Komattu AV, Delp SL. Internal rotation gait: A compensatory mechanism to restore abduction capacity decreased by bone deformity? *Dev Med Child Neurol* 1997;39:40–44.
13. Arnold AS, Salinas S, Asakawa DJ, Delp SL. Accuracy of muscle moment arms estimated from MRI-based musculoskeletal models of the lower extremity. *Comput Aided Surg* 2000;5:108–119.
14. Asakawa DJ, Blemker SS, Rab G, Bagley A, Delp SL. Three dimensional muscle tendon geometry after rectus femoris transfer. *J Bone Joint Surg Am* 2004;86–A:348–354.
15. Beals RK. Treatment of knee contracture in cerebral palsy by hamstring lengthening, posterior capsulotomy, and quadriceps mechanism shortening. *Dev Med Child Neurol* 2001;43:802–805.
16. Bhargava LJ, Pandy MG, Anderson FC. A phenomenological model for estimating metabolic energy consumption in muscle contraction. *J Biomech* 2004;37:81–88.
17. Bleck EE. *Orthopaedic Management in Cerebral Palsy*. London: Mac Keith Press, 1987.
18. Brand RA, Pedersen DR, Friederich JA. The sensitivity of muscle force predictions to changes in physiologic cross-sectional area. *J Biomech* 1986;19:589–596.
19. Campbell J, Ball J. Energetics: Application to the study and management of locomotor disabilities. Energetics of walking in cerebral palsy. *Orthop Clin North Am* 1978;9:374–377.
20. Chao EYS, Lynch JD, Vanderploeg MJ. Simulation and animation of musculoskeletal joint system. *J Biomech Eng* 1993;115:562–568.
21. Chow C, Jacobson D. Studies of human locomotion via optimal programming. *Math Biosci* 1971;10:239–306.
22. Damiano DL, Vaughan CL, Abel MF. Muscle response to heavy resistance exercise in children with spastic cerebral palsy. *Dev Med Child Neurol* 1995;37:731–739.
23. Davy DT, Audu ML. A dynamic optimization technique for predicting muscle forces in the swing phase of gait. *J Biomech* 1987;20:187–201.
24. Delp SL, Hess WE, Hungerford DS, Jones LC. Variation of rotation moment arms with hip flexion. *J Biomech* 1999;32:493–501.
25. Delp SL, Loan JP, Zajac FE, Topp EL, Rosen JM. An interactive graphics-based model of the lower extremity to study orthopaedic surgical procedures. *IEEE Trans Biomed Eng* 1990;37:757–767.
26. Delp SL, Loan JP. A computational framework for simulation and analysis of human and animal movement. *IEEE Comput Sci Eng* 2000;2:46–55.
27. Delp SL, Ringwelski DA, Carroll NC. Transfer of the rectus femoris: Effects of transfer site on moment arms about the knee and hip. *J Biomech* 1994;27:1201–1211.
28. Delp SL, Statler K, Carroll NC. Preserving plantar flexion strength after surgical treatment for contracture of the triceps surae: A computer simulation study. *J Orthop Res* 1995;13:96–104.
29. DeLuca PA, Ounpuu S, Davis RB, Walsh JH. Effect of hamstring and psoas lengthening on pelvic tilt in patients with spastic diplegic cerebral palsy. *J Pediatr Orthop* 1998;18:712–718.
30. Free SA, Delp SL. Trochanteric transfer in total hip replacement: Effects on the moment arms and force-generating capacities of the hip abductors. *J Orthop Res* 1996;14:245–250.
31. Friederich JA, Brand RA. Muscle fiber architecture in the human lower limb. *J Biomech* 1990;23:91–95.
32. Gage JR, Schwartz M. Pathological gait and lever-arm dysfunction. In: Gage JR, ed. *The Treatment of Gait Problems in Cerebral Palsy*. London: Mac Keith Press, 2004;180–204.
33. Gage JR. *Gait Analysis in Cerebral Palsy*. London: Mac Keith Press, 1991.
34. Gage JR. Treatment principles for crouch gait. In: Gage JR, ed. *The Treatment of Gait Problems in Cerebral Palsy*. London: Mac Keith Press, 2004;382–397.
35. Garner BA, Pandy MG. The obstacle-set method for representing muscle paths in musculoskeletal models. *Comput Methods Biomech Biomed Engin* 2000;3:1–30.
36. Gerritsen KG, van den Bogert AJ, Hulliger M, Zernicke RF. Intrinsic muscle properties facilitate locomotor control: A computer simulation study. *Motor Control* 1998;2:206–220.
37. Goldberg SR, Anderson FC, Pandy MG, Delp SL. Muscles that influence knee flexion velocity in double support: Implications for stiff-knee gait. *J Biomech* 2004;37:1189–1196.
38. Goldberg SR, Ounpuu S, Delp SL. The importance of swing phase initial conditions in stiff-knee gait. *J Biomech* 2003;36:1111–1116.
39. Hase K, Miyashita K, Ok S, Arakawa Y. Human gait simulation with a neuromusculoskeletal model and evolutionary computation. *J Vis Comput Animat* 2003;14:73–92.
40. Hase K, Yamazaki N. Computer simulation study of human locomotion with a three-dimensional entire-body neuro-musculoskeletal model (I. Acquisition of normal walking). *JSME Int J Ser C* 2002;45:1040–1072.
41. Higginson JS, Neptune RR, Anderson FC. Simulated parallel annealing within a neighborhood for optimization of biomechanical systems. *J Biomech* 2005;38:1938–1942.
42. Inman VT, Ralston HJ, Todd F. *Human Walking*. Baltimore: Williams & Wilkins; 1981.
43. Ito M, Akima H, Fukunaga T. In vivo moment arm determination using b-mode ultrasonography. *J Biomech* 2000;33:215–218.
44. Jonkers I, Stewart C, Spaepen A. The complementary role of the plantarflexors, hamstrings and gluteus maximus in the control of stance limb stability during gait. *Gait Posture* 2003;17:264–272.
45. Jonkers I, Stewart C, Spaepen A. The study of muscle action during single support and swing phase of gait: Clinical relevance of forward simulation techniques. *Gait Posture* 2003;17:97–105.
46. Kane T, Levinson D. *Dynamics: Theory and application*. New York: McGraw-Hill; 1985.
47. Kaplan ML, Heegaard JH. Predictive algorithms for neuromuscular control of human locomotion. *J Biomech* 2001;34:1077–1083.
48. Kepple TM, Siegel KL, Stanhope SJ. Relative contributions of the lower extremity joint moments to forward progression and support during gait. *Gait Posture* 1997;6:1–8.
49. Lieber RL, Steinman S, Barash IA, Chambers H. Structural and functional changes in spastic skeletal muscle. *Muscle Nerve* 2004;29:615–627.
50. Lloyd-Roberts GC, Jackson AM, Albert JS. Avulsion of the distal pole of the patella in cerebral palsy. *J Bone Joint Surg Br* 1985;67B:252–254.
51. Maganaris CN. In vivo measurement-based estimations of the moment arm in the human tibialis anterior muscle-tendon unit. *J Biomech* 2000;33:375–379.
52. McConville JT, Clauser CE, Churchill TD, Cuzzi J, Kaleps I. *Anthropometric Relationships of Body and Body Segment Moments of Inertia*. Report AFAMRL-TR-80-119. Air Force Aerospace Medical Research Laboratory, Wright-Patterson AFB, Ohio, 1980.
53. Mochon S, McMahon TA. Ballistic walking: An improved model. *Math Biosci* 1980;52:241–260.
54. Neptune R. Optimization algorithm performance in determining optimal controls in human movement analyses. *J Biomech Eng* 1999;121:249–252.
55. Neptune RR, Hull ML. Evaluation of performance criteria for simulation of submaximal steady-state cycling using a forward dynamic model. *J Biomech Eng* 1998;120:334–341.
56. Neptune RR, Kautz SA, Zajac FE. Contributions of the individual ankle plantar flexors to support, forward progression and swing initiation during walking. *J Biomech* 2001;34:1387–1398.
57. Neptune RR, Kautz SA. Knee joint loading in forward versus backward pedaling: Implications for rehabilitation strategies. *Clin Biomech* 2000;15:528–535.
58. Neptune RR, Zajac FE, Kautz SA. Muscle force redistributes segmental power for body progression during walking. *Gait Posture* 2004;19:194–205.

59. Neptune RR, Zajac FE, Kautz SA. Muscle mechanical work requirements during normal walking: The energetic cost of raising the body's center-of-mass is significant. *J Biomech* 2004;37:817–825.
60. Novacheck T, Trost J, Schwartz M. Intramuscular psoas lengthening improves dynamic hip function in children with cerebral palsy. *J Pediatr Orthop* 2002;22:158–164.
61. Ogihara N, Yamazaki N. Generation of human bipedal locomotion by a bio-mimetic neuro-musculo-skeletal model. *Biol Cybern* 2001;84:1–11.
62. Pandy MG, Anderson FC, Hull DG. A parameter optimization approach for the optimal control of large-scale musculoskeletal systems. *J Biomech Eng* 1992;114:450–460.
63. Pandy MG, Berme N. Quantitative assessment of gait determinants during single stance via a three-dimensional model: Part 1. Normal gait. *J Biomech* 1989;22:717–724.
64. Pandy MG, Berme N. Quantitative assessment of gait determinants during single stance via a three-dimensional model: Part 2. Pathological gait. *J Biomech* 1989;22:725–733.
65. Pandy MG, Garner BA, Anderson FC. Optimal control of non-ballistic muscular movements: A constraint-based performance criterion for rising from a chair. *J Biomech Eng* 1995;117:15–26.
66. Pandy MG, Zajac FE, Sim E, Levine WS. An optimal control model for maximum-height human jumping. *J Biomech* 1990;23:1185–1198.
67. Pandy MG. Computer modeling and simulation of human movement. *Ann Rev Biomed Eng* 2001;3:245–273.
68. Pandy MG. Simple and complex models for studying muscle function in walking. *Philos Trans R Soc Lond B Biol Sci* 2003;358:1501–1509.
69. Perry J, Antonelli D, Ford W. Analysis of knee-joint forces during flexed-knee stance. *J Bone Joint Surg Am* 1975;57A:961–967.
70. Perry J, Newsam C. Function of the hamstrings in cerebral palsy. In: Sussman MD, ed. *The Diplegic Child: Evaluation and Management. Rosemont*, IL: American Academy of Orthopaedic Surgeons, 1992;299–307.
71. Perry J. Distal rectus femoris transfer. *Dev Med Child Neurol* 1987;29:153–158.
72. Perry J. *Gait analysis: Normal and pathological function*. Thorofare, NJ: Slack Incorporated, 1992.
73. Piazza SJ, Delp SL. The influence of muscles on knee flexion during the swing phase of gait. *J Biomech* 1996;29:723–733.
74. Piazza SJ, Delp SL. Three-dimensional dynamic simulation of total knee replacement motion during a step-up task. *J Biomech Eng* 2001;123:599–606.
75. Rab GT, Muscle. In: Rose J, Gamble JG, eds. *Human Walking*. 2nd ed. Baltimore: Williams and Wilkins, 1994;101–121.
76. Ralston HJ. Energetics of human walking. In: Herman RM, Grillner S, Stein PSG, Stuart DG, eds. *Neural Control of Locomotion*. New York: Plenum Press, 1976;77–98.
77. Reimers J. Static and dynamic problems in spastic cerebral palsy. *J Bone Joint Surg Br* 1973;55-B:822–827.
78. Riley PO, Kerrigan DC. Torque action of two-joint muscles in the swing period of stiff-legged gait: A forward dynamic model analysis. *J Biomech* 1998;31:835–840.
79. Rodda J, Graham HK. Classification of gait patterns in spastic hemiplegia and spastic diplegia: A basis for a management algorithm. *Eur J Neurol* 2001;8(suppl 5):98–108.
80. Roosth HP. Flexion deformity of the hip and knee in spastic cerebral palsy: Treatment by early release of spastic hip-flexor muscles. *J Bone Joint Surg Am* 1971;53-A:1489–1510.
81. Rose J, Gamble J, Medeiros J, Burgos A, Haskell W. Energy expenditure index of walking for normal children and for children with cerebral palsy. *Dev Med Child Neurol* 1990;32:333–340.
82. Rosenthal RK, Levine DB. Fragmentation of the distal pole of the patella in spastic cerebral palsy. *J Bone Joint Surg Am* 1977;59A:934–939.
83. Schmidt DJ, Arnold AS, Carroll NC, Delp SL. Length changes of the hamstrings and adductors resulting from derotational osteotomies of the femur. *J Orthop Res* 1999;17:279–285.
84. Schutte LM, Rodgers MM, Zajac FE. Improving the efficacy of electrical stimulation-induced leg cycle ergometry: An analysis based on a dynamic musculoskeletal model. *IEEE Trans Rehab Eng* 1993;1:109–125.
85. Schwartz M, Lakin G. The effect of tibial torsion on the dynamic function of the soleus during gait. *Gait Posture* 2003;17:113–118.
86. Sheehan FT, Zajac FE, Drace JE. Using cine phase contrast magnetic resonance imaging to non-invasively study in vivo knee dynamics. *J Biomech* 1998;31:21–26.
87. Stout JL, Koop S. Energy expenditure in cerebral palsy. In: Gage JR, ed. *The Treatment of Gait Problems in Cerebral Palsy.* London: Mac Keith Press, 2004;146–164.
88. Sutherland DH, Cooper L, Daniel D. The Role of the Ankle Plantar Flexors in Normal Walking. *J Bone Joint Surg Am* 1980;62-A:354–363.
89. Sutherland DH, Cooper L. The pathomechanics of progressive crouch gait in spastic diplegia. *Orthop Clin North Am* 1978;9:143–154.
90. Sutherland DH, Davids JR. Common gait abnormalities of the knee in cerebral palsy. *Clin Orthop* 1993;288:139–147.
91. Sutherland DH, Santi M, Abel MF. Treatment of stiff-knee gait in cerebral palsy: A comparison by gait analysis of distal rectus femoris transfer versus proximal rectus release. *J Pediatr Orthop* 1990; 10: 433–441.
92. Taga G. A model of the neuro-musculo-skeletal system for anticipatory adjustment of human locomotion during obstacle avoidance. *Biol Cybern* 1998;78:9–17.
93. Thelen DG, Anderson FC, Delp SL. Generating forward dynamic simulations of movement using computed muscle control. *J Biomech* 2003;36:321–328.
94. van der Helm FCT, Rozendaall LA. Musculoskeletal systems with intrinsic and proprioceptive feedback. In: Winters JM, Crago PE, eds. *Biomechanics and Neural Control of Posture and Movement*. New York: Springer-Verlag, Inc., 2000;164–174.
95. van der Helm FCT, van Soest AJ. Planning of human motions: How simple must it be? In: Winters JM, Crago PE, eds. *Biomechanics and Neural Control of Posture and Movement*. New York: Springer-Verlag, Inc., 2000;373–381.
96. van Soest AJK, Casius LJR. The merits of a parallel genetic algorithm in solving hard optimization problems. *J Biomech Eng* 2003; 125:141–146.
97. Wickiewicz TL, Roy RR, Powell PL, Edgerton VR. Muscle architecture of the human lower limb. *Clin Orthop* 1983;275–283.
98. Wiley ME, Damiano DL. Lower-extremity strength profiles in spastic cerebral palsy. *Dev Med Child Neurol* 1998;40:100–107.
99. Wilson DL, Zhu Q, Duerk JL, Mansour JM, Kilgore K, Crago PE. Estimation of tendon moment arms from three-dimensional magnetic resonance images. *Ann Biomed Eng* 1999;27:247–256.
100. Winter DA. Overall principle of lower limb support during stance phase of gait. *J Biomech* 1980;13:923–927.
101. Winter DA. *The Biomechanics and Motor Control of Human Gait: Normal, Elderly, and Pathological.* Waterloo, Ontario, Canada: Waterloo Biomechanics, 1991.
102. Wright IC, Neptune RR, van den Bogert AJ, Nigg BM. The influence of foot positioning on ankle sprains. *J Biomech* 2000;33:513–519.
103. Yamaguchi GT, Zajac FE. A planar model of the knee joint to characterize the knee extensor mechanism. *J Biomech* 1989;22:1–10.
104. Yamaguchi GT, Zajac FE. Restoring unassisted natural gait to paraplegics via functional neuromuscular stimulation: A computer simulation study. *IEEE Trans Biomed Eng* 1990;37:886–902.
105. Zajac FE, Gordon ME. Determining muscle's force and action in multi-articular movement. *Exerc Sport Sci Rev* 1989;17:187–230.
106. Zajac FE, Neptune RR, Kautz SA. Biomechanics and muscle coordination of human walking part II: Lessons from dynamical simulations and clinical implications. *Gait Posture* 2003;17:1–17.
107. Zajac FE. Muscle and tendon: Properties, models, scaling, and application to biomechanics and motor control. *Crit Rev Biomed Eng* 1989;17:359–411.